Baltic Astronomy, vol. 14, 543–553, 2005.

RADIATIVE TRANSFER PROBLEM IN DUSTY GALAXIES: GALACTIC FOG ENGINE

D. Semionov and V. Vansevičius
Institute of Physics, Savanoriu 231, Vilnius LT-02300, Lithuania

Received 2005 October 1; revised 2005 December 28

Abstract. A new code for the evaluation of light absorption and scattering by interstellar dust grains is presented. The radiative transfer problem is solved by using ray-tracing algorithm in a self-consistent and highly efficient way. The code demonstrates performance and accuracy similar or better than that of previously published results, achieved using Monte-Carlo methods, with an accuracy better than $\sim 1\%$ for most cases. The intended application of the code is spectrophotometric modeling of disk galaxies, however, it can be easily applied to other cases that require a detailed spatial evaluation of scattering, such as circumstellar disks and shells containing both point and extended light sources.

Key words: radiative transfer – ISM: dust, extinction

1. PROBLEM STATEMENT

The purpose of the developed radiative transfer problem solving code is to model spatial and spectral energy distribution (SED) observed in disk galaxies. The nature of this problem requires 'self-consistency' of a solution – the resulting SED of a model must depend only on SEDs of stellar sources and assumed properties of dust without any preconditioning on light and attenuation distribution within galaxy (Takagi et al. 2003).

While galaxies in general are complex objects with three-dimensional (3D) distribution of radiation and matter, in most cases they are dominated by axial symmetry (2D), allowing significant simplification of the model geometry. However, the model should account for presence of macroscopic structure within galaxies, possibly including elements having other symmetry, such as bars and spiral arms (2D+).

Most present-day astrophysical radiative transfer codes employ either a Monte-Carlo (MC, e.g., Ciardi et al. 2001) or a ray-tracing (RTR, e.g., Razoumov & Scott 1999) methods. Some of implementations of these methods were compared by Baes & Dejonghe (2001) for 1D and by Dullemond & Turolla (2000) for 2D cases. The RTR approach allows the optimization of a solution for a given system geometry (Vansevičius et al. 1997), which was the main reason to use it as a basis for the developed Galactic Fog Engine (hereafter 'GFE'), a program for a self-consistent solution of the radiative transfer problem in dusty media with primarily axi-symmetrical geometry. The GFE iteratively solves a discrete bidirectional radiative transfer problem, producing intensity maps of the model under arbitrary inclination at a given wavelength set.

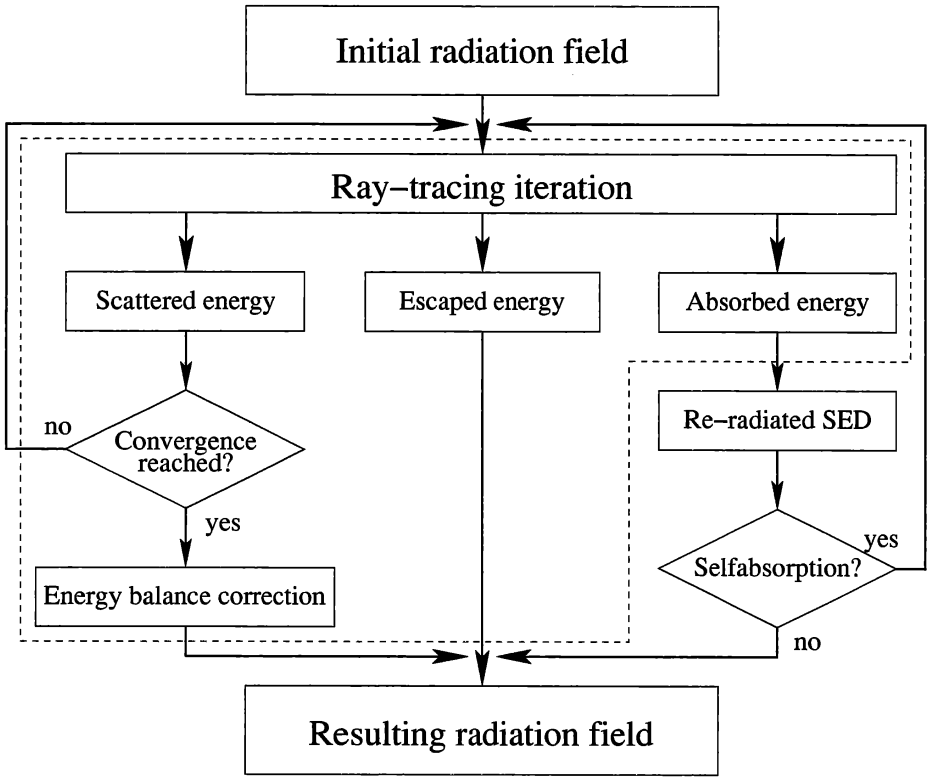

Fig. 1. The flowchart of the Galactic Fog Engine.

This paper concentrates on radiative transfer in ultraviolet to near infrared wavelength range assuming exclusively coherent scattering, therefore in most equations the wavelength dependence will be omitted. The algorithm and model geometry used are described in section 2. In section 3 we discuss the computational accuracy of the model, assessing the errors introduced by model subdivision and interpolation quality. Finally, in section 4 we summarize the results, underlining the accuracy and application limits of our method and compare them to other codes/algorithms used for similar purpose.

2. MODEL DESCRIPTION

2.1. Model geometry

The foundation of the iterative evaluation of radiative transfer equation was laid out by Henyey (1937). By solving the radiative transfer equation the initial system radiation field is separated into the following: the escaped energy that reaches an external observer; the energy absorbed by grains and eventually emitted as thermal radiation with appropriate SED; and the scattered energy (Figure 1). The solution is then repeated, taking the scattered energy as the initial distribution for the next iteration and accumulating the resulting escaped and absorbed energy, until certain convergence criteria are met, using either a fixed number of iterations, or leaving the scattered energy below a specified threshold. After the convergence is reached, the dust temperature is calculated from the absorbed en-

ergy distribution. If it is necessary to take into consideration self-scattering of thermal radiation by dust grains, the resulting emission SED can be employed as an input into scattering evaluation loop, and the process repeated until the final radiative energy distribution is obtained, and then used to produce SED as seen by an external observer.

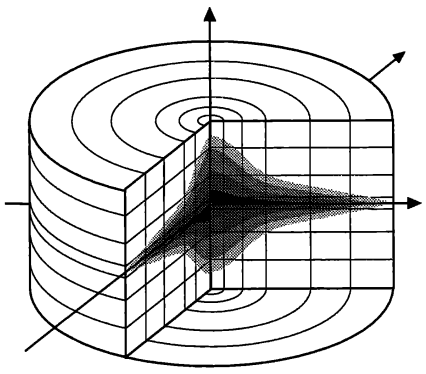

Fig. 2. Model geometry.

Calculations are performed within a cylinder with a radius r_m and height above the midplane z_m, which is subdivided into a set of layers of concentric, internally homogeneous rings ('bins') of arbitrary radial and vertical thickness (Figure 2). Since the linear extent of each individual light source (star) is negligible compared to the size of the system, it is possible to solve the radiative transfer problem considering every volume element of the model having both attenuating (light scattering and absorption by interstellar dust) and emitting (light emission by stars and thermal radiation of dust particles) properties per unit volume, defining for each ring denoted by indexes i and j its total absorption $k' = \kappa(r_i, z_j)$ and emissivity $j' = j(r_i, z_j, \alpha, \delta)$, combined from internal light sources and energy scattered within its volume, with angles α and δ defining the direction of radiation propagation.

2.2. Discrete radiative transfer equation

GFE uses static ray-casting geometry, determining the set of rays that ensures a required degree of sampling of the model volume. The sampling of the model is controlled by setting the minimum number of rays required to pass through each ring under every inclination considered. Ray-casting also can be done adaptively by adding more rays to the parts of the model where there is a significant difference in sampled energy between the neighboring rays until this difference is reduced below a specified value (in this work a 20% difference threshold is used). However, as these rays are not a part of the initially precalculated geometry, this can result in significant increase in computing time.

If the viewing solid angle containing each ray can be held small, the radiative transfer along these rays can be solved as in the case of plane-parallel homogeneous layer for a series of intervals traversing rings until crossing the outer boundary of the model. The classical form of one-dimensional radiative transfer equations can be written as (Chandrasekhar 1960):

$$\frac{dI}{ds} = -\kappa I + j + \kappa \frac{\omega}{4\pi} \int I \Phi d\Omega, \tag{1}$$

where Φ and ω denote the scattering phase function and albedo, and κ and j are the absorption and emissivity coefficients of the medium. We have used the Henyey & Greenstein (1941) scattering phase function parametrization with asymmetry parameter g:

$$\Phi(\theta) = \frac{1 - g^2}{(1 + g^2 - 2g\cos\theta)^{3/2}}. \tag{2}$$

In a form suitable for a computer implementation, an incident intensity on a given point for a light path separated into n intervals of length l_i, numbered outwards from that point, is

$$I_{\rm inc} = \sum_{i=1}^{n} \left(\prod_{j=1}^{i-1} e^{-k'_j l_j} \right) \frac{j'_i}{k'_i} \left(1 - e^{-k'_i l_i} \right). \quad (3)$$

Similarly, the intensity of radiation scattered with albedo ω from a given direction $(\alpha : \delta)$ into all other directions within a certain ray interval (denoted by index "1") is

$$I_{1,\alpha,\delta} = \omega j'_1 l_1 - \omega \left(1 - e^{-k'_1 l_1} \right) \left[\frac{j'_1}{k'_1} - \sum_{i=2}^{n} \left(\prod_{j=2}^{i-1} e^{-k'_j l_j} \right) \frac{j'_i}{k'_i} \left(1 - e^{-k'_i l_i} \right) \right]. \quad (4)$$

When considering an azimuthally inhomogeneous model configuration (3D case), each ring is subdivided into the required number of azimuthal segments. The number and directions of rays cast through the system have to be modified accordingly to include the new sets of rays in azimuthal direction, however, the ray-tracing part of the algorithm is unchanged. The computational time-scales are $N_{\rm bin}^{3/2} \times \log N_{\rm bin}$ for 2D and $N_{\rm bin}^{4/3} \times \log N_{\rm bin}$ for 3D cases. The application of this code is not restricted to the systems with dispersed sources and absorbers, the algorithm being easily extended to include the treatment of point sources and interaction between radiation field and surfaces of macroscopic objects.

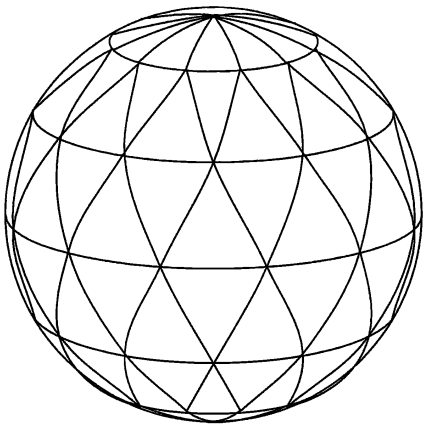

Fig. 3. An example of the reference direction structure used for the iso-latitude triangulation of the scattering phase function using $N_{\rm RD} = 62$ (cf. Figure 6).

Since the angular distribution of radiation at each point in the model is non-isotropic, it must be described using a numerical phase function (matrix), providing the radiation intensity towards a set of predefined reference directions ('RDs') described by angular coordinates $(\alpha_0 : \delta_0)$. A number of ways exists to distribute RDs on a sphere, however, those methods that produce a set of RDs arranged in iso-latitude rows are the most preferable in this particular model geometry, allowing both efficient storage and retrieval of scattered intensity and fast rotation of the phase matrix around the model Z-axis. The memory requirements and the overall algorithm's performance have also to be taken into consideration.

GFE implements the following RD distribution methods: an iso-latitude triangulation (hereafter 'ILT', Figure 3), HEALPix[1] (Górski et al. 1999) and HTM[2]

[1] http://www.eso.org/science/healpix/

[2] http://www.sdss.jhu.edu/htm/

(Kunszt et al. 2001). For all triangulation schemes the radiation intensity towards a given point can be interpolated between the three nearest RDs using either 'flat' or 'spherical' weights. In this work we will limit ourselves to the models utilizing ILT scheme, the comparison between all implemented methods will be presented elsewhere (Semionov & Vansevičius, in preparation).

3. COMPUTATION ACCURACY

3.1. Standard model

The problem often encountered applying numerical methods is error accumulation. In case of iterative ray-tracing it arises from sampling and interpolation errors. The source of sampling errors is incomplete or/and inadequate spatial sampling of the system, while interpolation errors are related primarily to the accuracy of scattering phase function approximation. Both error types independently affect every ray traced through the system, thus the accumulated error increases with the increasing number of bins and rays. This makes oversampling undesirable not only due to increasing computational time, but also for a reason of minimizing numerical errors.

As a measure of method's quality we use a defect in energy balance $E_{\rm err}$ defined as a percentage of total energy radiated within system $E_{\rm tot}$

$$E_{\rm err} = \frac{E_{\rm tot} - E_{\rm abs} - E_{\rm sca} - E_{\rm esc}}{E_{\rm tot}}, \tag{5}$$

where $E_{\rm esc}$, $E_{\rm abs}$ and $E_{\rm sca}$ are the parts of a total radiated energy that escaped the system or was absorbed and remained to be scattered within the system, respectively.

In the following discussion we will use, unless specified otherwise, the "standard" model: a cylinder with radius to height above midplane ratio of $r_m/z_m = 5$, divided into $N_z = 21$ layers consisting of $N_r = 26$ rings with the appropriate ring and layer width and thickness scaled as $\Delta r_i = 1.2\Delta r_{i-1}$ and $\Delta z_i = 1.2\Delta z_{i-1}$ respectively, with adaptive ray-casting algorithm. Within it the dust and stellar density are distributed according to a double-exponential law:

$$\rho(r, z) = \rho_0 e^{-r/r_0} e^{-z/z_0} \tag{6}$$

with effective scale-length $r_0 = 0.2r_m$ for both stars and dust and effective scale-height $z_0^{\rm stars} = 0.1z_m$ for stars and $z_0^{\rm dust} = 0.05z_m$, respectively. The effective scale-height ratio $z_0^{\rm stars}/z_0^{\rm dust} = 2$ was chosen over a "well-mixed" model with both stars and dust having the same scale-length and -height since it represents a larger challenge to the radiative transfer code. The central optical depth to the model center in V passband measured perpendicularly to the central plane was assumed to be $\tau(V) = 2.5$. Dust optical properties were computed using Laor & Draine (1993) model, representing the scattering phase function using ILT scheme with 366 RDs. All models were computed with seven scattering iterations, of these the first three were performed exactly and the remaining four – using iteration scaling approximation (Semionov & Vansevičius 2005b).

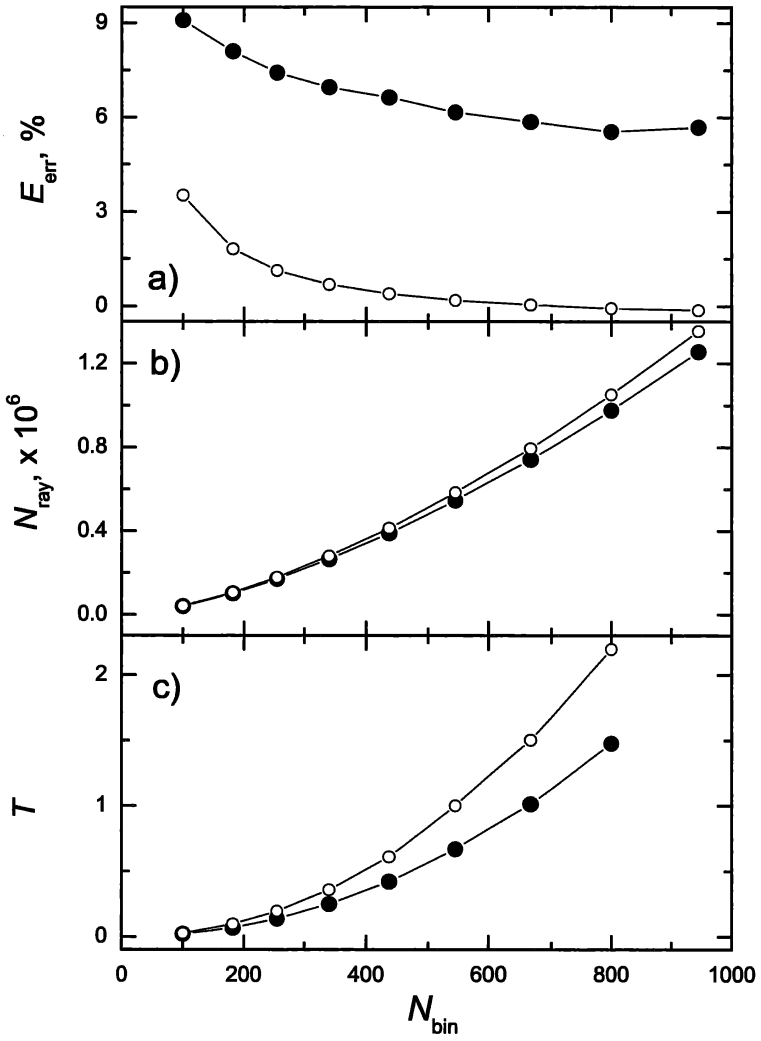

Fig. 4. Effect of model subdivision on overall energy balance and computational performance for static (line with solid symbols) and adaptive (line with open symbols) ray-casting. The dependence of energy defect $E_{\rm err}$ (in percent, panel a), total number rays $N_{\rm ray}$ (panel b) and computing time T relative to the standard model (panel c) are displayed.

3.2. Model volume subdivision and sampling

In order to establish the effects of model subdivision and sampling on the numerical error, we have performed two sets of tests using the standard model as a starting point. First, the number of rings N_r and layers N_z was varied while keeping the required number of ray-ring intersections ($N_{\rm rri}$) constant, the results obtained for both static and adaptive ray-casting schemes. Subsequently, fixing the standard model subdivision, we alter the $N_{\rm rri}$ using adaptive ray-casting method.

The subdivision test results, presented in Figure 4, show gradual decrease of model energy defect with increasing number of model elements $N_{\rm bin} = N_r \times N_z$. After a certain value of $N_{\rm bin}$, the improvement in model accuracy becomes very slow, requiring large amounts of additional computing time and making further

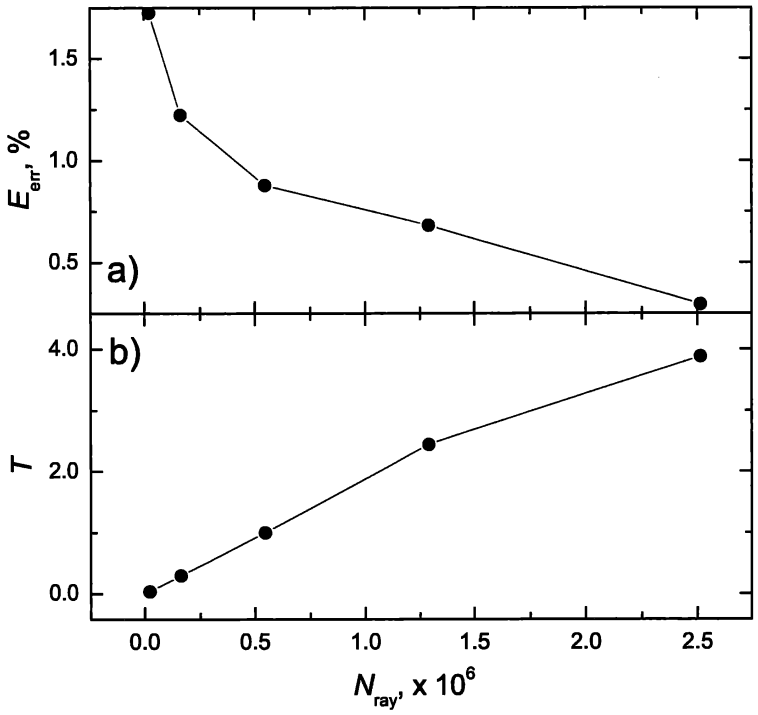

Fig. 5. Dependence of the energy defect $E_{\rm err}$ (panel a) and relative computing time T (panel b) on the number of rays for adaptive ray-casting in the standard model.

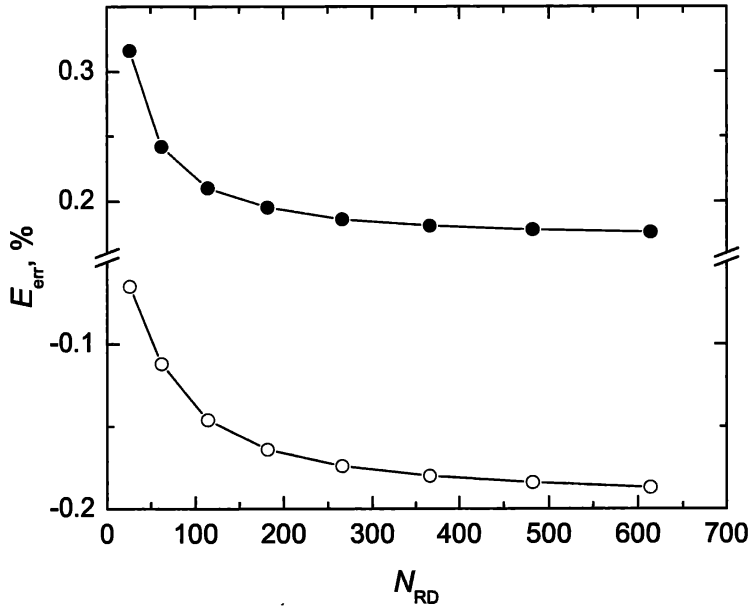

Fig. 6. Energy defect $E_{\rm err}$ dependence on the number of reference directions for V ($\lambda = 550$ nm, line with solid symbols) and FUV ($\lambda = 165$ nm, line with open symbols) passbands.

increase of $N_{\rm bin}$ superficial. In contrast to that, as can be seen in Figure 4a, the adaptive ray-casting algorithm offers a significant improvement in accuracy over static ray-casting, which makes its use preferable despite the associated increase in computing time (up to 35%).

The energy defect dependence on the ray-casting density, shown in Figure 5a, displays similar pattern as that in the previous test, with errors rapidly decreasing with increasing number of rays $N_{\rm ray}$. However, the computing time (shown in Figure 5b) and memory requirements grow significantly faster than the improving of the model accuracy. As with model subdivision, the optimal ray-casting density must be determined by considering both the accuracy and computational resources constrains.

3.3. Interpolation of the scattering phase function

Increasing the number of RDs provides a more exact representation of the scattering phase function and angular distribution of scattered light, decreasing the associated interpolation errors. To test the sensitivity of model results to the number of RDs when interpolating scattering phase functions with different values of asymmetry parameter g, we have compared several models at $\lambda = 165$ nm and 550 nm (V filter) wavelengths with $N_{\rm RD}$ gradually increasing it from 26 to 614. The results, presented on Figure 6, show a trend of energy defect quickly approaching a "saturated" value, after which a further increase of $N_{\rm RD}$ does not produce a noticeable improvement in model accuracy for all wavelengths. The energy defect in *FUV* ($g_{165} = 0.62$) behaves similarly to the one in V passband ($g_V = 0.46$), however, it approaches the "saturated" value more slowly. According to these results, the choice of $N_{\rm RD} = 366$, used in the standard model, can be considered optimal for an ILT interpolation scheme of the scattering phase function at all wavelengths from the FUV to near-infrared range.

However, it is also important to ensure that alteration of the numerical algorithm parameters does not change the resulting radial intensity profile of the galaxy model. In this case, while a numerical defect may be small, confirming the model energy balance correctness, the insufficient sampling of the scattering phase function will have the effect of decreasing the proper value of the asymmetry parameter g_λ (effectively making scattering more isotropic), altering radial intensity profile of the model up to several percent (Semionov & Vansevičius 2005a).

3.4. Dust optical properties

Another important aspect of a numerical radiative transfer solution is its sensitivity to variations in scattering parameters: albedo ω and scattering phase function asymmetry parameter g. Model accuracy and stability for different ω and g values place a constraint on the wavelength range where a given method can be applied. To test the sensitivity of the model accuracy to the optical properties of dust grains we have performed two tests, separately varying each of these two parameters while keeping the other one fixed at a value of 0.5.

The dependence of the overall model accuracy on the scattering asymmetry parameter g, assuming $\omega = 0.5$, is shown in Figure 7a. The total energy defect shows a significant variation with increasing g up to the limit imposed by the angular scattering phase function grids used in the calculations ($N_{\rm RD} = 366$), after which the scattered energy errors render the results invalid. The effect of the variation of dust grain albedo ω assuming $g = 0.5$ is shown in Figure 7b. Within

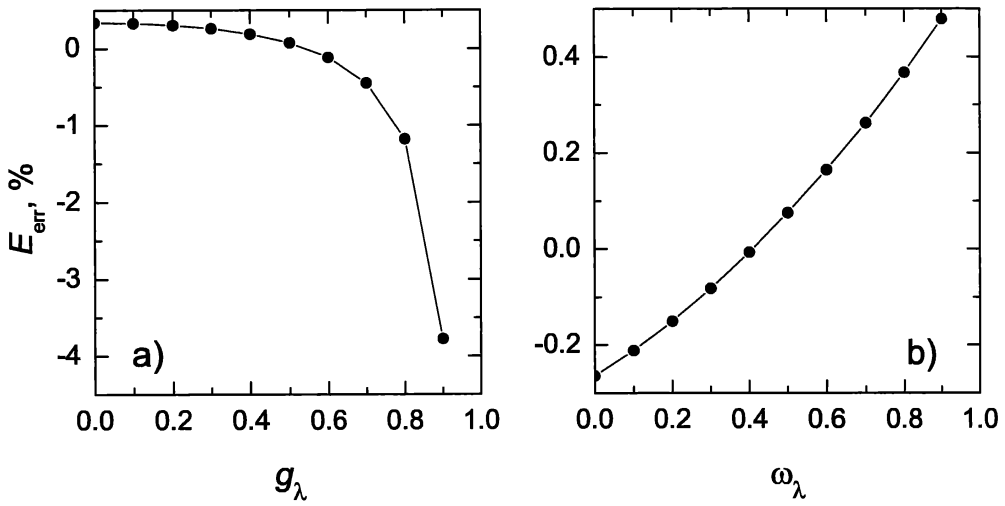

Fig. 7. Energy defect dependence on the dust optical properties: the scattering phase function asymmetry parameter g (panel a, for $\omega = 0.5$) and albedo ω (panel b, for $g = 0.5$).

the range of ω values, applicable to astrophysical dust grains, those errors stay in acceptable limits, and do not influence the stability of the solution.

Figure 7 illustrates the relation between two main error sources inherent to RTR codes: error accumulation during successive ray-tracing iterations and the scattering phase function interpolation. Finite arithmetic precision results in the loss of a small amount of radiation energy during each ray-tracing, thus increasing $E_{\rm err}$ (making it more positive) as $E_{\rm sca}$ becomes less than $E_{\rm tot} - E_{\rm abs} - E_{\rm esc}$ (eq. 5). Increasing albedo leaves more and more radiation energy in higher-order iterations ($E_{\rm sca} = 0.16E_{\rm tot}$ after three iterations with $\omega = 0.9$), leading to significant error accumulation, while in case of no scattering, $\omega = 0$, the energy balance and light distribution are fully accounted for within the first iteration and no error accumulation takes place.

When using a limited number of RDs to store and retrieve scattered light distribution, interpolation errors are introduced. Due to a form of scattering phase function these errors overestimate the amount of scattered light (resulting in negative values of $E_{\rm err}$) and increase with increasing values of asymmetry parameter g for a given number of RDs, reaching zero only for isotropic scattering ($g = 0$). The combination of these two effects can be seen in Figure 7a: initially, at $g = 0$, the energy defect is a small positive number, showing the energy losses due to ray-tracing error accumulation. Then, as the value of g increases, the interpolation errors, overestimating the amount of scattered light, gradually begin to dominate the model energy balance until the scattering phase function becomes too elongated to be correctly represented using a given number of RDs, and the RT solution breaks down.

4. SUMMARY

The code described in this paper has shown the flexibility and performance satisfying the requirements for the models of the global radiative transfer in dusty galaxies (Semionov & Vansevičius 2002). It has been successfully applied to model

both integral and position-dependent SEDs of several galaxies, some of the first results presented in Semionov et al. (2003).

The main limiting factor affecting the applicability of the described code is the scattering asymmetry parameter g_λ. In order to correctly treat scattering with g_λ approaching 1, the number of required reference directions rises sharply, affecting both the performance and the accuracy of the method. For a "standard" disk galaxy model described in this paper, a satisfactory convergence is obtained for g_λ in the [-0.8; 0.8] range which represents well the optical properties of typical astrophysical grains from microwave up to extreme ultraviolet wavelengths.

Other model properties, such as optical depth τ_λ and the relative amount of scattered radiation (dependent on albedo ω_λ) seem to have relatively little effect on the quality of the solutions. However, models with large optical depth (of the order of a few 100s), particularly having steep dust distribution gradients, require a significant amount of computing time and computer memory.

The results of the extensive testing of the developed code, presented in this article, primarily address the accuracy dependence of the model on the numerical parameters of the algorithm: model geometry – subdivision of the model, ray-casting density – number of rays traced through the model and their distribution, and scattering phase function interpolation. While a straightforward increase of each of these quantities, $N_{\rm bin}$, $N_{\rm ray}$ and $N_{\rm RD}$ does improve model accuracy, it does not appear to be the optimal strategy as increasing these parameters beyond certain values leads to a very slow decrease of associated numerical errors at the expense of rapid increase of computing time and computer memory requirements.

Instead, it appears to be advantageous to search for optimal values of these parameters providing the best attainable accuracy to the required computing resources ratio. At the same time, the method itself can be further improved by increasing the arithmetic precision in storage and retrieval of scattered light matrices and by searching for the best interpolation scheme with good performance and small numerical errors. As an example, changing the GFE code from single to double precision has decreased the average numerical errors approximately by a factor of three in comparison with the results reported earlier (Semionov & Vansevičius 2002), at the cost of moderate increase of the computing time and memory required (approximately by 25%).

ACKNOWLEDGMENTS. The authors express their gratitude to Rima Stonkutė for her help in performing the computations and data handling. The computations, presented in this paper, were in part performed on computers of the Astronomical Data Analysis Center of the National Astronomical Observatory of Japan. This work was supported by a Grant of the Lithuanian State Science and Studies Foundation. We are thankful to T. Viik for the report and important comments.

REFERENCES

Baes M., Dejonghe H. 2001, MNRAS, 326, 722

Chandrasekhar S. 1960, *Radiative Transfer*, New York, Dover

Ciardi B., Ferrara A., Marri S., Raimondo G. 2001, MNRAS, 324, 381

Dullemond C., Turolla R. 2000, A&A, 360, 1187

Górski K., Hivon E., Wandelt B. 1999, in *Proceedings of the MPA/ESO Cosmology*

Conference "Evolution of Large-Scale Structures" eds. A. Banday, R. Sheth & L. Da Costa, PrintPartners Ipskamp, NL, 37

Henyey L. 1937, ApJ, 85, 107

Henyey L., Greenstein J. 1941, ApJ, 93, 70

Kunszt P., Szalay A., Thakar A. 2001, in *Mining the Sky: Proceedings of the MPA/ESO/MPE workshop, Garching*, eds. A. Banday, S. Zaroubi & M. Bartelmann, Springer-Verlag, Berlin-Heidelberg, 631

Kylafis N., Bahcall J. 1987, ApJ, 317, 637

Laor A., Draine B. 1993, ApJ, 402, 441

Pascucci I., Wolf S., Steinacker J., Dullemond C., Henning Th., Niccolini G., Woitke P., Lopez B. 2004, A&A, 417, 793

Razoumov A., Scott D. 1999, MNRAS, 309, 287

Razoumov A., Michael M., Abel T., Scott D. 2002, ApJ, 572, 695

Semionov D., Vansevičius V. 2002, Baltic Astronomy, 11, 537

Semionov D., Stonkutė R., Vansevičius V. 2003, Baltic Astronomy, 12, 633

Semionov D. 2003, *Spectrophotometric Evolution of Dusty Disk Galaxies*, Inst. of Theoretical Physics and Astronomy, Vilnius, PhD thesis

Semionov D., Vansevičius V. 2005a, Baltic Astronomy, 14, 235

Semionov D., Vansevičius V. 2005b, Baltic Astronomy, 14, 245

Vansevičius V., Arimoto N., Kodaira K. 1997, ApJ, 474, 623

Takagi T., Vansevičius V., Arimoto N. 2003, PASJ, 55, 385